1-1-2010

Noise transfer functions of mode-locked semiconductor laser

Sangyoun Gee

Peter J. Delfyett
University of Central Florida

Noise transfer functions of mode-locked semiconductor laser

Sangyoun Gee,[1,*] and Peter J. Delfyett[2]

[1]*Advanced Photonics Research Institute, Gwangju Institute of Science and Technology, Gwangju, 500-712, Korea*
[2]*College of Optics and Photonics, Center for Research and Education in Optics & Lasers (CREOL), University of Central Florida, Orlando, FL 32816-2700, USA*
**sgee@gist.ac.kr*

Abstract: The noise behavior of mode-locked semiconductor ring laser, including timing jitter, and pulse energy fluctuation are investigated using the notion of a noise transfer function. Numerical simulation predicts that semiconductor mode-locked lasers have very complex structure in the transfer function which is confirmed experimentally by corresponding noise measurements.

OCIS codes: (140.4050) Mode-locked lasers; (120.3940) Metrology.

References and links

1. H. A. Haus, and A. Mecozzi, "Noise of Mode-locked lasers," J. Quantum Electron. **29**(3), 983–996 (1993).
2. H. A. Haus, M. Margalit, and C. X. Yu, "Quantum noise of a mode-locked laser," J. Opt. Soc. Am. B **17**(7), 1240–1256 (2000).
3. L. A. Jiang, M. E. Grein, H. A. Haus, and E. P. Ippen, "Noise of Mode-locked Semiconductor lasers," J. Sel. Top. Quantum Electron. **7**(2), 159–167 (2001).
4. D. R. Hjelme, and A. R. Mickelson, "Theory of Timing Jitter in Actively Mode-locked lasers," J. of Quantum Electron. **28**(6), 1594–1606 (1992).
5. P. T. Ho, "Phase and Amplitude Fluctuations in a Mode-Locked laser," J. Quantum Electron. **21**(11), 1806–1813 (1985).
6. J. K. Wahlstrand, J. T. Willits, T. R. Schibli, C. R. Menyuk, and S. T. Cundiff, "Quantitative measurement of timing and phase dynamics in a mode-locked laser," Opt. Lett. **32**(23), 3426–3428 (2007).
7. J. K. Wahlstrand, J. T. Willits, C. R. Menyuk, and S. T. Cundiff, "The quantum-limited comb lineshape of a mode-locked laser: fundamental limits on frequency uncertainty," Opt. Express **16**(23), 18624–18630 (2008).
8. E. L. O'Neill, "Introduction to statistical optics," (Dover Pub., Mineola, N.Y. 1991)
9. S. Gee, S. Ozharar, J. J. Plant, P. W. Juodawlkis, and P. J. Delfyett, "Intracavity dispersion effect on timing jitter of ultralow noise mode-locked semiconductor based external-cavity laser," Opt. Lett. **34**(3), 238–240 (2009).
10. F. Rana, R. Ram, and H. A. Haus, "Quantum noise of actively mode-locked lasers with dispersion and amplitude/phase modulation," J. Quantum Electron. **40**(1), 41–56 (2004).
11. S. Ozharar, I. Ozdur, F. Quinlan, and P. J. Delfyett, "Jitter reduction by intracavity active phase modulation in a mode-locked semiconductor laser," Opt. Lett. **34**(5), 677–679 (2009).
12. J. C. Diels, and W. Rudolph, "Ultrashort laser pulse Phenomena," (Academic, New York, 1996)
13. M. Y. Hong, Y. H. Chang, A. Dienes, J. P. Heritage, and P. J. Delfyett, "Subpicosecond Pulse Amplification in Semiconductor Laser Amplifiers: Theory and Experiment," J. Quantum Electron. **30**(4), 1122–1131 (1994).

1. Introduction

Theories of mode-locked laser noise have been developed by many researchers in the past. These theories can be modeled in both time and frequency domains. The time domain approach is employed by Haus et al. where a linearized noise equation is driven from a master equation of mode-locking [1–3]. Haus's work is based on soliton perturbation theory and, therefore, presumes temporally hyperbolic secant shaped pulses as output. On the other hand, one example of the frequency domain approach can be found from Hjelme et al. where a master equation of mode-locking is used for each longitudinal mode and then perturbation is applied to obtain an equation of noise [4,5]. In this case, an output Gaussian pulse shape was assumed. Both of these approaches have analytic solutions for the noise spectral density, often having a Lorentzian shape $1/\left(\Omega^2+\gamma^2\right)$ or a product of Lorentzian shape

#119583 - $15.00 USD Received 5 Nov 2009; revised 15 Dec 2009; accepted 16 Dec 2009; published 4 Jan 2010

$1/\left(\Omega^2+\gamma_1^2\right)\left(\Omega^2+\gamma_2^2\right)$ noise spectra, and are excellent in understanding the general behavior of mode-locked laser noise.

Noise behavior of many practical mode-locked lasers can be understood using these approaches. For example, Haus's model works especially well for Ti:sapphire mode-locked lasers and mode-locked fiber lasers relying on the Kerr effect. However, there are many other types of mode-locked lasers which do not fall into those categories, e.g., semiconductor mode-locked lasers. Owing to large nonlinearities and gain, mode-locked semiconductor lasers generate pulses with quite complex shapes typically accompanied with a chirp. These pulse shapes are neither Gaussian nor hyperbolic secant. Therefore the justification of applying the above theories on mode-locked semiconductor lasers is rather weak, although these theories provide excellent insights about qualitative noise behavior.

Another approach to study the noise behavior of mode-locked lasers independent of the type of mode-locking mechanism was proposed and demonstrated by monitoring the linearized response of the mode-locked pulse parameters to perturbations, such as pump power fluctuation [6,7]. For five parameters of mode-locked lasers; the laser gain Δg, the pulse energy Δw, the central frequency $\Delta\omega$, the pulse timing Δt, and the phase $\Delta\theta$, the relation between the response and the perturbation was assumed as,

$$\frac{d\mathbf{v}}{dt}=-\mathbf{A}\cdot\mathbf{v}+\mathbf{S} \tag{1}$$

where $\mathbf{v}=\left(\Delta g,\Delta w,\Delta\omega,\Delta t,\Delta\theta\right)$, $\mathbf{S}$ is a vector of noise sources, and $\mathbf{A}$ is a matrix defining the linear response. The approach is to determine $\mathbf{A}$, then for a given $\mathbf{S}$, the full laser noise behavior can be understood from the above relation. This approach is useful to study many general cases of mode-locked lasers, however as Eq. (1) suggests, it assumes that responses decay exponentially in time, which will result in Lorentzian like power spectra of noise. This condition may not be able to explain more complicate response behavior, often observed in semiconductor mode-locked lasers. In order to handle these cases, no assumption is made about the response dynamics except that it is linear, causal, and stable [8]. In this case, the response of a laser parameter to a noise source can be generally written as,

$$\mathbf{v}_i\left(t\right)=\int_{-\infty}^{t}\mathbf{h}_{i,j}\left(t-t'\right)\cdot\mathbf{s}_j\left(t'\right)dt' \tag{2}$$

Or in the frequency domain,

$$\mathbf{V}_i\left(\Omega\right)=\mathbf{H}_{i,j}\left(\Omega\right)\cdot\mathbf{S}_j\left(\Omega\right) \tag{3}$$

where $h_{i,j}(t)$ and $H_{i,j}(\Omega)$ are impulse response and transfer function of *i*th laser parameter to *j*th noise source component, respectively. This expression is especially useful, because for semiconductor laser cases, $S_j(\Omega)$ can be easily generated by driving electronics while $V_i(\Omega)$ can be monitored by a fast photo-detector and an electrical spectrum analyzer. $H_{i,j}(\Omega)$ can be obtained from the measured $S_j(\Omega)$ and $V_j(\Omega)$, and once $H_{i,j}(\Omega)$ is obtained then all the laser noise behavior can be understood in the same way proposed in [6]. In this paper, we have measured the pulse timing and the pulse energy response to the laser cavity length fluctuation and pump current fluctuation for a semiconductor mode-locked ring laser. The measurement results shows rather complicated structure in their power spectra, which has never been reported by any of previous researchers. A numerical simulation of the small signal response of mode-locked laser shows qualitative match with the experimental results and suggests that the complex structures in the response spectra are owing to anharmonic ringing of the laser response relaxation.

It should be noted there has been excellent progress in the development of ultralow noise mode-locked semiconductor laser, yielding relative timing jitter under 500 attoseconds (1 Hz ~1 MHz) owing to careful cavity engineering [9]. In addition, there has been the development

#119583 - $15.00 USD Received 5 Nov 2009; revised 15 Dec 2009; accepted 16 Dec 2009; published 4 Jan 2010

of novel theory [10] and subsequent verification that careful understanding of intracavity nonlinearities can be exploited to generate ultralow noise pulse trains with lower noise than what would be considered the optimal laser cavity design [11]. As a result, the determination of the noise transfer function becomes paramount in the design of optimized laser cavity for ultralow noise pulse train generation.

2. Numerical simulation of small signal response dynamics

The schematic diagram of the mode-locked laser studied in this paper is shown in Fig. 1. The gain medium is a semiconductor optical amplifier (SOA) biased at 500 mA DC. The mode-locking was achieved by active modulation of a Mach-Zehnder electro-optic modulator driven by a microwave synthesizer at 10 GHz. The laser cavity is primarily composed of fiber pig tails of various optical components, which contributes net negative group velocity dispersion (GVD). The schematic diagram of the numerical model of the mode-locked laser dynamics is shown in Fig. 2. Each optical component is treated as a lumped element and the pulse evolution is traced in the same order as the actual pulse travels in the experimental configuration. The cavity dispersion, the spectral filter, and the self phase modulation (SPM) were treated in the frequency domain while the intensity modulator, gain dynamics, and output coupler were treated in the time domain. This approach is similar to the split-step Fourier method in the sense that the simulation is done either in time or in frequency domain alternately. Numerical models for each component are shown below [12,13]. The mathematical expressions for each lumped elements are shown in Eq. (4) through Eq. (8). The time span for the simulation was 100 ps with 1024 sample points. Simulation parameters are summarized in Table 1.

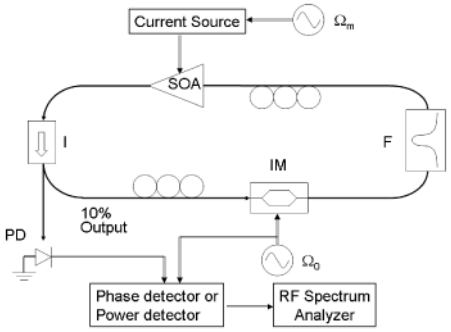

Fig. 1. Schematic diagram of the experimental setup.PD; photo detector, IM; intensity odulator, F; optical filter, Ω_0; mode-locking freq., Ω_m; external modulation freq.

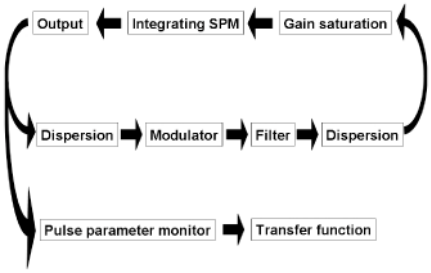

Fig. 2. Schematic diagram of the simulation.

Gain saturation

$$E_{out}(t) = E_{in}(t) \cdot \sqrt{\frac{\exp\left(2\sigma_g \cdot W(t)\right)}{\exp\left(-a_g\right) - 1 + \exp\left(2\sigma_g \cdot W(t)\right)}} \quad (4)$$

#119583 - $15.00 USD Received 5 Nov 2009; revised 15 Dec 2009; accepted 16 Dec 2009; published 4 Jan 2010

$$\textit{Integrating SPM} \qquad E_{out}(t) = E_{in}(t)\cdot\exp\left(i\cdot s\cdot W(t)\right) \tag{5}$$

$$\textit{GVD} \qquad E_{out}(\omega) = E_{in}(\omega)\cdot\exp\left[i\cdot\frac{k''}{2}\cdot L\cdot(\omega-\omega_0)^2\right] \tag{6}$$

$$\textit{Filter} \qquad E_{out}(\omega) = E_{in}(\omega)\cdot\exp\left[-\left(\frac{\omega-\omega_0}{\Delta\omega}\right)^2\right] \tag{7}$$

$$\textit{Modulator} \qquad E_{out}(t) = E_{in}(t)\cdot\cos\left(\frac{\pi}{2}\cdot\frac{V(t)}{V_\pi}\right) \tag{8}$$

where $W(t)=\int_{-\infty}^{t}\left|E_{in}(t')\right|^2 dt'$ is the pulse energy, and σ_g, a_g, s, k'', L, $\Delta\omega$, and V_π are gain cross section, amplification coefficient, phenomenological coefficient of SPM, GVD of fiber, optical fiber length, spectral filter bandwidth, and π phase shift voltage of the modulator, respectively. The validity of the simulation can be claimed by considering the similarity in spectral shape between a simulation and a measurement.

Table 1. Simulation Parameters

Parameter	Symbol	Value
Gain cross section	σ_g	9.88 x10^{-3} /pJ
Amplification coefficient	a_g	4.8
Phenomenological coefficient of SPM	s	1.186 x 10^{-1} /pJ
GVD of fiber	k''	12.4 ps/nm-km
Fiber length	L	15 m
Spectral filter bandwidth	$\Delta\omega$	1.1 x 10^{13} /s
V_π of the modulator	V_π	5.5 V

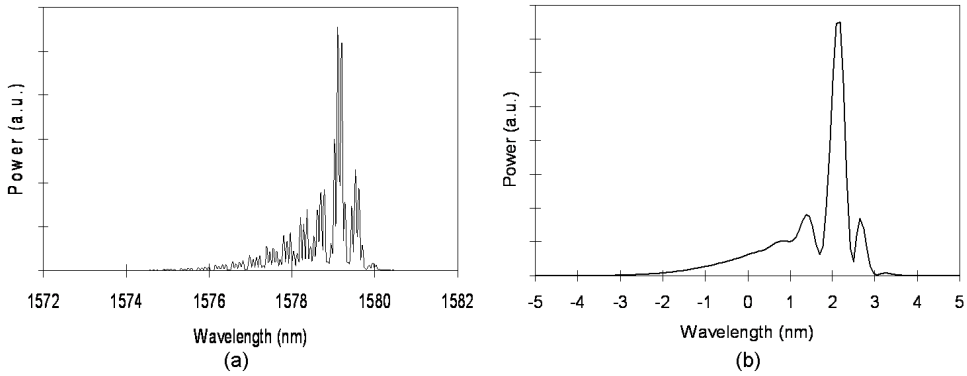

Fig. 3. Optical spectra of mode-locked laser output: (a) the measured spectrum, (b) the simulated spectrum.

Figure 3 shows the measured and simulated optical spectra of laser output. The measured spectrum shows triangular shaped spectrum with a sharp peak on the long wavelength side. The needle-like sharp structure in the spectrum is partially resolved longitudinal modes. The simulated spectrum shows the same trends in the spectral shape except that it has lower resolution owing to the limited number of samples. This unique spectral shape leads to a unique temporal pulse shape as well. The simulated temporal intensity profile and the instantaneous frequency offset are shown in Fig. 4. From the figure, it appears as if the pulse is composed of two parts. The leading portion possesses a well defined pulse with large down chirp, while the trailing portion contains a broad peak with small chirp. When compared to the optical spectrum, the leading portion is attributed to the spectrum spanning the short and mid

#119583 - $15.00 USD Received 5 Nov 2009; revised 15 Dec 2009; accepted 16 Dec 2009; published 4 Jan 2010

wavelength range, while the trailing portion of the pulse is attributed to the sharp peak on the long wavelength side. The overall sign of the chirp is negative; however, these two portions have two different slopes. This aspect has been confirmed by intensity autocorrelation measurements. The laser output pulses were sent to a dual grating pulse compressor before they are detected by an autocorrelator. The autocorrelation measurement shows that there are two different components of the pulse; each part compresses at different amount of dispersion compensation. This feature of complex pulse shape is not caused by a single effect but by the combined effect of SPM, cavity dispersion, gain saturation, etc. For example, the inclusion of dispersion compensation fiber into the cavity can cause a dramatic change in spectral shape. It is this nature of complex pulse shape that prevents one to utilized Haus's or Hjelme's theory of noise to semiconductor lasers.

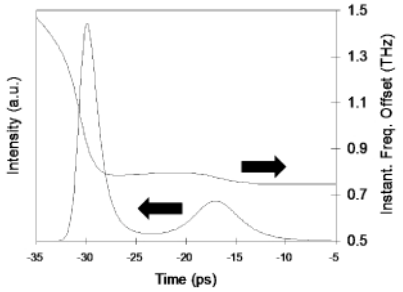

Fig. 4. Temporal intensity profile of the pulse and instantaneous frequency offset.

The simulation procedure of the small signal response to an impulse from a noise source is described below. First, by iteration of many round trip of the pulse in the cavity, a steady state pulse shape is achieved. Then, an impulse to one of the laser's noise source is applied: cavity length change, pump current change, cavity loss change, etc. In the third step, the iteration of the pulse round trip in the cavity is resumed and laser parameters, such as pulse timing, pulse energy, and center frequency are monitored (Fig. 2). These results provide the impulse response functions $h_{i,j}(t)$, the Fourier transform then gives the transfer functions $H_{i,j}(\Omega)$. The simulated response functions and transfer functions are shown in Fig. 5, and Fig. 6 for an SOA gain change impulse, and an impulsive cavity length change, respectively.

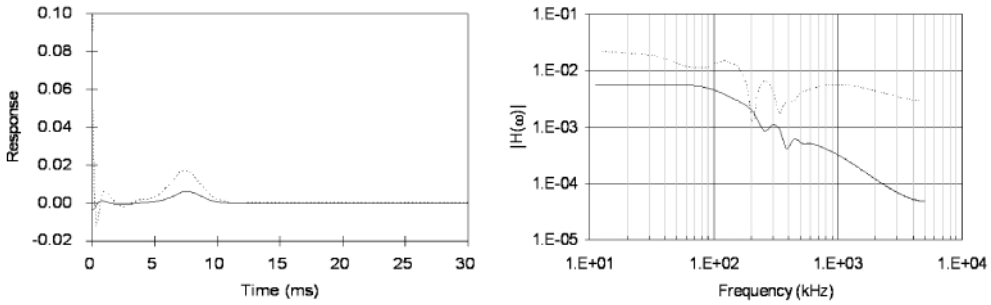

Fig. 5. Responses for 10% of gain change: solid line for pulse timing, and dotted line for pulse energy.

#119583 - $15.00 USD Received 5 Nov 2009; revised 15 Dec 2009; accepted 16 Dec 2009; published 4 Jan 2010

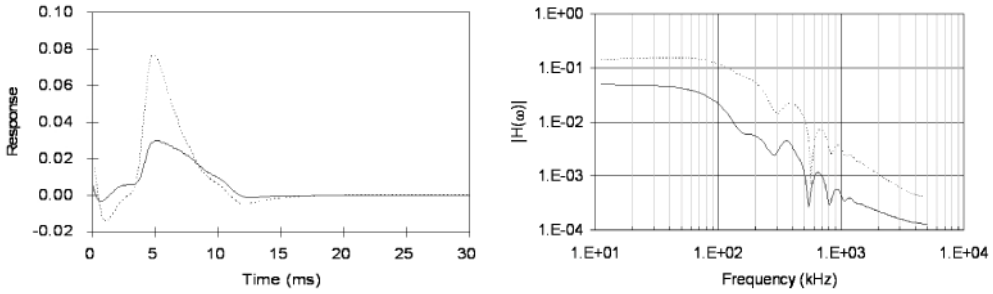

Fig. 6. Responses for 1% cavity length change: solid line for pulse timing, and dotted line for pulse energy.

The impulse responses show a relaxation oscillation behavior. Unlike a typical relaxation oscillation which is composed of a harmonic oscillation with an exponential decay of amplitude, these relaxations show complex decaying dynamics which includes overshooting and a reduction of the oscillation frequency in time. As a result, the transfer functions also show several peaks in addition to a typical $1/\left(\Omega^2+\gamma^2\right)$ shape. It is this behavior that is the unique contribution of this work in comparison to previously reported works.

3. Experimental measurements of transfer functions

In order to confirm the simulation results, transfer functions of each impulse response are measured. The schematic of the set up is shown in Fig. 1. For the gain change response, a small amount of AC component is added to a DC bias current to SOA. This AC component is provided by a tunable RF source. The responses of the laser against this AC component shows up as a spur in both amplitude noise, and phase noise measurement of photo current utilizing a power detector, and a phase detector, respectively. The strength of the spur is monitored as the frequency Ω_m of the AC component is varying, which gives the transfer function. The results are shown in Fig. 7 along with the simulation results. A common trend in both the measurement result and the simulated result is a plateau at the low frequency end followed by a roll-off around 100 kHz. In addition, several peaks occur between 100 kHz and 1 MHz for both measurement ((a), (b)) and simulation ((a'), (b')); the position of the peaks have a one to one correspondence to each other. The locations of these peaks are related to the oscillating frequency of the response signal in the time domain. The fact that the simulation and experiment both show similar value for the locations of these peaks implies that the time scale of the dynamics in the simulation is accurate. However, the slope of the roll-off at high offset frequency shows large difference. The exact origin of these discrepancies needs further investigation to understand. One potential explanation for the slower decay of the simulated results at high frequency could be the discretization error of the numerical simulation, which produces white noise and dominates the high frequency range in the transfer function.

#119583 - $15.00 USD Received 5 Nov 2009; revised 15 Dec 2009; accepted 16 Dec 2009; published 4 Jan 2010

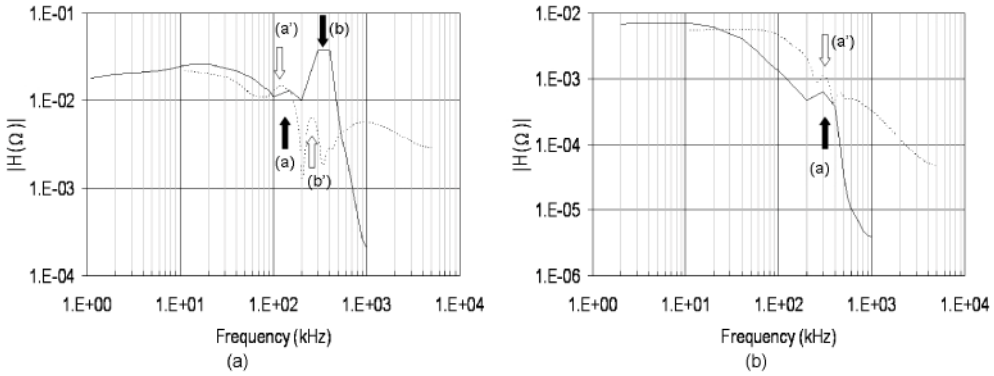

Fig. 7. The measured (solid line) and simulated (dotted line) transfer functions for 10% of gain change: (a) the pulse energy response, (b) the pulse timing response.

The response of the laser to the cavity length change can be investigated in a similar manner as the gain change case except it is the cavity length that is modulated. However the cavity length modulation requires mechanical moving parts and is not trivial to achieve. On the other hand, the mode-locking frequency Ω_0 from a RF source can be easily modulated by one of built-in function from a commercial product. For a small amount of frequency detuning $\Delta\Omega$ from Ω_0, the effective cavity length change ΔL can be obtained from a simple relationship; $\Delta\Omega / \Omega_0 = -\Delta L / L_0$, where the L_0 is the cavity length. Therefore the mode-locking frequency Ω_0 was modulated by a small amount instead of the cavity length modulation in the current experiment. Again, a noise spur is generated at a frequency of a rate of the frequency modulation, not at the amount of frequency deviation $\Delta\Omega$. The strength of the spur is monitored as the rate of the frequency modulation is varying, which gives the transfer function. Figure 8 shows the measurement results along with the simulation results. The trend is the same as the responses to the gain change case.

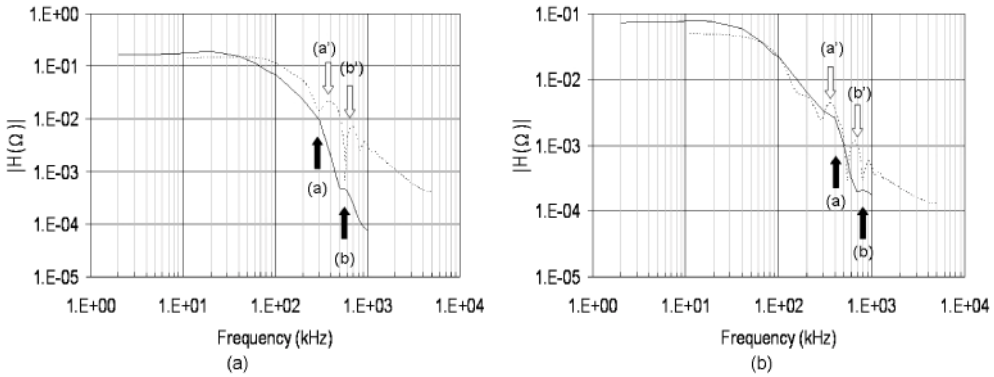

Fig. 8. The measured (solid line) and simulated (dotted line) transfer functions for 1% of cavity length change: (a) the pulse energy response, (b) the pulse timing response.

4. Conclusions

Dynamic responses of the mode-locked semiconductor laser in terms of the pulse energy, and the pulse timing against the gain fluctuation, and the cavity length fluctuation are investigated both by numerical simulations and experimental measurements. The simulation predicts unconventional relaxation behavior in the impulse response including non-monotonic decay of the amplitude and a slowing down of the fluctuation frequency, which is in contrast to common relaxation oscillations where the amplitude envelope decays exponentially while it oscillates at a fixed frequency. The fluctuation leads to a spectral modulation in the transfer

#119583 - $15.00 USD Received 5 Nov 2009; revised 15 Dec 2009; accepted 16 Dec 2009; published 4 Jan 2010

function. Noise spur measurements of the gain or the cavity length modulated laser provide the experimental means to measure the transfer functions. These measurement results confirmed the general trend predicted by the numerical simulation, especially by the agreement of the location of the peaks in the transfer functions. Once the transfer functions of all laser parameters are known, the complete noise behavior of a mode-locked laser can be reconstructed and this numerical model can be a useful tool to understand other interesting aspects of mode-locked laser noise, such as mode-partition noise, super-mode noise, minimization of noise, etc. It is anticipated that the determination of these noise transfer functions will allow the design of an optimized mode-locked cavity for ultralow noise pulse train generation from a semiconductor diode gain based system with sub 100 attosecond jitter.

Acknowledgments

This work was supported by the Korean Research Foundation Grant funded by the Korean Government (MOEHRD, Basic Research Promotion Fund) (KRF-2007-313-C00291), the second phase of the Brain Korea 21 Program, and (Photonics2020) research project through a grant provided by the Gwangju Institute of Science and Technology in 2009.

#119583 - $15.00 USD Received 5 Nov 2009; revised 15 Dec 2009; accepted 16 Dec 2009; published 4 Jan 2010